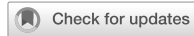




ARTICLE



Wide-field OCTA quantified peripheral nonperfusion areas predict the risk of subclinical neovascularization

An-Lun Wu^{1,2}, Yukun Guo^{1,3}, Tristan T. Hormel¹, Christina J. Flaxel¹, Merina Thomas¹, Steven T. Bailey¹, Dong-Wouk Park¹, Yali Jia^{1,3} and Thomas S. Hwang¹

© The Author(s), under exclusive licence to The Royal College of Ophthalmologists 2025

PURPOSE: To demonstrate the capabilities of single-shot widefield swept-source OCT angiography (SS-OCTA) in detecting subclinical retinal neovascularization (RNV), quantifying nonperfusion areas (NPAs), and exploring the relations between NPAs and subclinical RNV in eyes graded as nonproliferative diabetic retinopathy (NPDR).

METHODS: Eyes clinically graded as moderate to severe NPDR underwent SS-OCTA imaging. Expert graders identified subclinical RNV, defined as vessels with a flow signal above the internal limiting membrane on OCTA that are not visible on dilated fundus examination. This identification was based on a combination of *en face* OCT, *en face* OCTA, and cross-sectional OCTA overlaid on OCT. NPA index was calculated as a percentage of automatically quantified NPA over the area in the posterior pole, the mid-periphery, and the total imaged area.

RESULTS: Totally 37 eyes, including 21 had severe NPDR and 16 had moderate NPDR. Subclinical RNV was present in 14 eyes (37.8%). The eyes with RNV had significantly higher mid-peripheral and total NPA indices but not in the posterior region (mid-peripheral NPA: $31.97\% \pm 7.02\%$ vs. $24.80\% \pm 6.60\%$, $p = 0.041$; total NPA: $27.96\% \pm 6.36\%$ vs. $21.61\% \pm 5.65\%$, $p = 0.046$; all values are reported as mean \pm standard deviation). The total NPA index showed the highest diagnostic accuracy for subclinical RNV detection (AUC: 0.761; 95% CI, 0.592–0.929, with a sensitivity of 64.3% and a specificity of 87% at a cutoff value of 28.84%).

CONCLUSION: Widefield SS-OCTA can detect subclinical RNV. The eyes with higher mid-peripheral NPA indices are more likely to have subclinical RNV, indicating that the NPA index may be a useful biomarker for identifying eyes at risk of RNV.

Eye; <https://doi.org/10.1038/s41433-025-03891-2>

INTRODUCTION

Diabetic retinopathy (DR) is the leading cause of preventable blindness among working-age adults globally, driven by chronic hyperglycemia leading to progressive microvascular damage in the retina [1, 2]. As DR progresses, retinal nonperfusion and ischemia contribute to the development of retinal neovascularization (RNV), a hallmark of proliferative diabetic retinopathy (PDR), which is associated with sight-threatening complications such as vitreous hemorrhage and tractional retinal detachment. The extent of retinal nonperfusion area (NPA) has been shown to increase with the severity of DR classification, indicating a pathological relationship between microvascular ischemia and disease progression, ultimately driving DR toward more advanced stages [3, 4].

Currently, the standard of care for detecting RNV is careful dilated ophthalmoscopy or color fundus photography according to the American Academy of Ophthalmology Preferred Practice Patterns on DR [5]. Fluorescein angiography (FA) is usually used to identify suspected but clinically obscure RNV and is not routinely used as part of the regular examination of patients with diabetes. As a result, we may overlook subtle preclinical microvascular changes that are not clinically suspected. Optical coherence tomography angiography (OCTA) [6, 7] offers advantage of effectively revealing vascular abnormalities including

neovascularization on the retinal surface by providing non-invasive, high-resolution, three-dimensional visualization of retinal blood flow in relation to retinal structure, enabling the identification of subtle RNV in DR cases that were undetectable via clinical examination or color fundus photography [8, 9]. This is a safer, faster, and less expensive alternative to FA for routine RNV screening, particularly in more advanced cases of non-proliferative diabetic retinopathy (NPDR), where the cost and risks associated with FA may outweigh the potential benefit of identifying unsuspected RNV. Our group demonstrated that combining *en face* OCT, *en face* OCTA, and cross-sectional OCTA significantly improves detection accuracy, allowing for the detection of occult RNV with high sensitivity [10]. Additionally, we characterized distinct morphologies of RNV, identifying sprouts and fronds, with longitudinal studies highlighting their evolution and potential as biomarkers of disease progression [11]. In this study, we define subclinical RNV as the identification of vessels with a flow signal above the internal limiting membrane (ILM) on OCTA, which are undetectable through standard clinical examinations.

Despite these advances, most studies utilizing OCTA have been constrained by small fields of view that can overlook mid-peripheral lesions where early RNV often originates [12]. The advent of single-shot widefield OCTA offers a transformative

¹Casey Eye Institute, Oregon Health & Science University, Portland, OR, USA. ²Department of Ophthalmology, Mackay Memorial Hospital, Hsinchu, Taiwan. ³Department of Biomedical Engineering, Oregon Health & Science University, Portland, OR, USA. email: hwangt@ohsu.edu

Received: 8 March 2025 Revised: 4 June 2025 Accepted: 12 June 2025

Published online: 02 July 2025

opportunity to investigate retinal changes more comprehensively [13]. Moreover, a robust deep-learning-based quantification of NPAs, which correlate with DR severity and are not affected by imaging artifacts, has been validated [14, 15]. These innovations provide the opportunity to integrate the detection of RNV and quantification of NPA using OCTA widefield imaging to improve the detection and understanding of early neovascular changes in DR. This study explores the relationship between NPA and the presence of RNV using a single-shot widefield OCTA.

METHOD

Study participants

The data reported in this cross-sectional analysis from a prospective observational study (NIH grant R01 EY035410) at the Casey Eye Institute, Oregon Health & Science University, from December 2023, through September 2024. The study adhered to the tenets of the Declaration of Helsinki and complied with the Health Insurance Portability and Accountability Act of 1996. Approval was obtained from the Institutional Review Board of Oregon Health & Science University, and written informed consent was obtained from all participants.

We recruited consecutive patients with a clinical diagnosis of moderate to severe NPDR without other concurrent ocular pathology based on findings observable upon dilation with funduscopic examination using the International Clinical Diabetic Retinopathy Disease Severity Scale [16]. All participants underwent comprehensive ophthalmic examinations, including standard Early Treatment of Diabetic Retinopathy Study (ETDRS) visual acuity testing, intraocular pressure measurement, slit-lamp examination, and standard dilated fundus examination using slit-lamp biomicroscopy with a 90-diopter (D) or 78D lens, and indirect ophthalmoscopy [5]. If both eyes of a patient met the eligibility criteria, one eye was randomly selected for inclusion.

Image acquisition and analysis

Imaging was performed using a pre-market commercial 200-kHz swept-source OCTA system (DREAM OCT, Intalight Inc.) with 1050 nm central wavelength. Each eye was centered on the fovea during imaging, and scans were acquired using the OCTA volumetric scans of 26×21 mm with 1536×1240 sampling density. These settings provided a field of view up to an eye angle of 130 degrees, enabling high-resolution imaging of both the posterior pole and mid-peripheral retina.

We used different segmentation strategies for *en face* OCT vs. OCTA to optimize the identification of RNV as previously reported in our earlier studies [10, 11]. For *en face* OCT, the vitreoretinal interface slab was defined as the region bounded by the ILM and a position 30 μm anterior to the ILM. For *en face* OCTA, the slab was defined as the region bounded by the ILM and a position 300 μm anterior to the ILM. RNV was identified by the presence of flow signals above the ILM on cross-sectional OCTA (overlaid on OCT), corresponding to epiretinal hyperreflective material on *en face* OCT or abnormal flow signals on *en face* OCTA. The presence of RNV was determined by two trained graders (AW and YG) and confirmed by an expert grader (TSH) using a combination of *en face* OCT, *en face* OCTA, and cross-sectional OCTA generated with commercially available software.

To perform image processing for NPA quantification, the entire retinal layer was segmented from the ILM to the outer plexiform layer using a guided bidirectional graph search algorithm that segmented the retinal layer boundaries [17]. A maximum projection method was used to project OCTA data within the slab to visualize an *en face* angiogram [18]. An NPA map was created using a deep-learning-based algorithm to automatically quantify NPAs as in previously reported methods [14, 19–21]. The total NPA index is defined as the percentage of quantified NPA over the total imaged area. We also analyzed the NPA index separately for the posterior pole, defined as the region centered on the fovea, with the radius defined by the distance from the fovea to the optic disc center, and the mid-periphery, defined as the area outside this circle. The foveal avascular zone was excluded from these calculations. The location of each RNV lesion was documented as either within the posterior pole or the mid-periphery of the retina, based on the same criteria, enabling further spatial analysis of lesion distribution.

Statistical analysis

Data were analyzed using SPSS Statistics (version 26.0; IBM Corp, Armonk, NY). Descriptive statistics are reported as mean \pm standard deviation, and

counts with percentages were used to summarize demographic and baseline clinical characteristics as appropriate. Fisher's exact test or Chi-squared test was applied to compare categorical variables, while independent *t*-tests were used for continuous variables. An area under the receiver operating characteristic curve was analyzed to evaluate the diagnostic performance of NPA indices in classifying eyes with or without subclinical RNV. Sensitivity, specificity, and area under the curve values were calculated for posterior pole, mid-peripheral, and total NPA indices. The optimal threshold for the NPA index associated with subclinical RNV detection was determined using the Youden Index. This threshold was then used to identify eyes at high risk for subclinical RNV development, with regional comparisons performed to determine the most diagnostically valuable metric. All *P* values were two-tailed, and a value of <0.05 was considered statistically significant.

RESULTS

Of 38 initially enrolled eyes, 37 (97.4%) had capillary details with sufficient image quality for analysis, and one was excluded due to significant motion artifacts and signal loss. Of these, 21 eyes (56.8%) were clinically graded as severe NPDR, and 16 eyes (43.2%) as moderate NPDR. The average age of participants was 56.9 ± 10.8 years, with a gender distribution of 14 males and 23 females. Among the study participants, 27 (73%) were treatment naïve, defined as having no prior panretinal photocoagulation or anti-VEGF injections. The participant characteristics are summarized in Table 1.

Subclinical RNV was identified in 14 eyes (37.8%) using widefield SS-OCTA. Among these eyes, 6 cases (42.9%) exhibited RNV exclusively in the mid-periphery. Of the 14 eyes with subclinical RNV, 8 eyes (57.1%) were clinically graded as severe NPDR, while 6 eyes (42.9%) were graded as moderate NPDR. A comparison of the clinical characteristics between eyes with and without subclinical RNV revealed no significant differences (Table 2).

The mean NPA indices (\pm SD) of the eyes with subclinical RNV for the posterior pole, mid-peripheral retina, and total retinal regions were $3.49 \pm 3.25\%$, $31.97 \pm 7.02\%$, and $27.96 \pm 6.36\%$, respectively. The corresponding NPA indices for eyes without RNV were $1.74 \pm 2.11\%$, $24.80 \pm 6.60\%$, and $21.61 \pm 5.65\%$. The total and mid-peripheral NPA indices were significantly higher for the eyes with RNV compared to those without ($p < 0.05$), but not

Table 1. Demographic and clinical characteristics of the study participants.

Parameters	(n = 37)
Age, years	56.9 ± 10.8
Sex, n (male/female)	14/23
Laterality, n (right/left)	12/25
Most recent HbA1c, %	8.0 ± 2.2
Duration of DM, years	19.4 ± 8.0
Type 1 DM, n (%)	6 (16.2)
DR stage	
Moderate NPDR, eyes (%)	16 (43.2)
Severe NPDR, eyes (%)	21 (56.8)
Treatment naïve, eyes (%)	27 (73.0)
Previous treatment	
Intravitreal VEGF injection, eyes	8
Panretinal photocoagulation, eyes	0
Both, eyes	2
logMAR Visual Acuity	0.08 ± 0.18

Continuous variables are expressed as mean \pm standard deviation; categorical variables are presented as counts and percentages.

DM diabetes mellitus, DR diabetic retinopathy, NPDR non-proliferative diabetic retinopathy, VEGF vascular endothelial growth factor, logMAR logarithm of the minimum angle of resolution.

Table 2. Characteristics between eyes with and without subclinical retinal neovascularization.

Parameters	RNV(+) (n = 14)	RNV(−) (n = 23)	P value
Age, years	56.9 ± 11.2	56.9 ± 10.8	0.929
Sex			0.804 ^a
Female	8 (57.1)	15 (65.2)	
Male	6 (42.9)	8 (34.8)	
Laterality			0.367 ^a
Right	10 (71.4)	15 (65.2)	
Left	4 (28.6)	8 (34.8)	
Most recent HbA1c, %	8.9 ± 2.9	7.5 ± 1.5	0.684
Duration of DM, years	20.4 ± 8.7	18.8 ± 7.8	0.568
DM Type			0.561 ^a
Type I	1 (7.1)	5 (21.7)	
Type II	13 (92.9)	18 (78.3)	
DR stage			1.000 ^a
Moderate NPDR	6 (42.9)	10 (43.5)	
Severe NPDR	8 (57.1)	13 (56.5)	
Treatment naïve			1.000 ^a
No	2 (14.3)	8 (34.8)	
Yes	12 (85.7)	15 (65.2)	
logMAR Visual Acuity	0.14 ± 0.25	0.04 ± 0.11	0.445

Continuous variables are expressed as mean ± standard deviation; categorical variables are presented as counts and percentages.

RNV retinal neovascularization, HbA1c Hemoglobin A1c, DM diabetes mellitus, DR diabetic retinopathy, NPDR non-proliferative diabetic retinopathy, logMAR logarithm of the minimum angle of resolution.

^aFisher's exact test.

the posterior NPA index. Representative images of eyes with and without subclinical RNV are shown in Fig. 1, along with corresponding nonperfusion maps featuring color-coded delineations of different retinal regions.

When comparing eyes with subclinical neovascularization at disc (NVD) vs. subclinical neovascularization elsewhere (NVE) only eyes, subclinical NVD eyes had significantly higher mid-peripheral and total NPA indices of $35.82 \pm 5.86\%$, and $31.46 \pm 4.93\%$ vs. $29.48 \pm 5.50\%$, and $25.67 \pm 5.45\%$ ($p < 0.05$). The posterior NPA indices for the two groups were not significantly different at $4.77 \pm 3.50\%$ for NVD eyes and $2.49 \pm 2.75\%$ NVE-only eyes. The comparison of NPA indices among the groups is presented in Table 3.

The total NPA index had the highest AUC for identifying eyes with RNV, with an AUC of 0.761 (95% CI, 0.592–0.929), compared to 0.758 (95% CI, 0.591–0.924) for the mid-peripheral NPA index and 0.630 (95% CI, 0.424–0.837) for the posterior pole NPA index (Fig. 2). Based on the Youden index, the optimal cutoff value for the total NPA index was 28.8%, achieving a specificity of 87% and a sensitivity of 64.3% for detecting subclinical RNV.

DISCUSSION

This study demonstrated the utility of single-shot widefield OCTA in detecting subclinical RNV in a significant number of eyes clinically graded as moderate or severe NPDR. In nearly half of these eyes, the subclinical RNV was found exclusively in the mid-periphery. Additionally, we demonstrated the value of peripheral NPA quantification using deep-learning algorithms, which

predicted the presence of subclinical RNV better than the NPA assessment of the posterior pole. These findings highlight the diagnostic benefit of widefield OCTA in detecting clinically undetectable RNV, offering a clear advantage and potentially leading to significant improvements in DR management.

Our study demonstrated a higher detection rate of subclinical RNV compared to previously published rates of 15%–28% reported in our prior work [9–11]. While some of the differences may be explained because the current study included only the eyes graded as moderate to severe NPDR, the increased detection rate in this series may also be attributed to the use of a larger field of view. Although prior studies have utilized montage views of OCTA scans to achieve a widefield view (~17 × 17 mm) [9–11], our single-shot widefield imaging in this study captures a broader retinal area (26 × 21 mm), extending anatomically closer to the posterior edge of the vortex vein ampulla [22]. This approach has the potential to provide more diagnostic information in a non-invasive and efficient manner. This reinforces the desirability of widefield OCTA as a tool for detecting proliferative changes in its earlier stages, and exploring these preclinical abnormalities could facilitate better characterization of disease severity and identify new therapeutic targets.

The total and mid-peripheral NPA indices were significantly higher in eyes with subclinical RNV compared to those without, highlighting the critical role of retinal nonperfusion in DR pathophysiology and its potential as a biomarker for disease severity. FA-identified nonperfusion has been recognized as a hallmark of retinal ischemia, correlating with microvascular damage and an increased likelihood of neovascularization [23, 24]. However, FA-based assessments are invasive and can pose challenges in accurately quantifying ischemia, especially when microvascular leakage is present. OCTA enables the quantitative detection of non-perfused areas without the confounding effects of leakage [25]. Studies have validated that OCTA demonstrates superior sensitivity in detecting NPAs compared to FA and provides repeatable and reproducible automated metrics for evaluating retinal ischemia [8, 26]. In this study, we calculated NPAs using the inner retinal slab because the superficial vascular complex and deep capillary plexus progressively merge as they extend beyond the posterior pole [27]. This anatomical configuration makes capillary dropout more reliably visualized using *en face* OCTA of the entire inner retinal slab [14]. Our previous research has demonstrated that NPAs detected using OCTA are significantly associated with DR severity, progression, and treatment requirements [28]. These findings indirectly support our results, highlighting the potential of single-shot widefield OCTA as a non-invasive and accessible tool capable of detecting pathologic features that may not be readily visible to clinicians.

Retinal NPA location also appears to be relevant. In our study, nearly half of the eyes with RNV had lesions exclusively in the mid-periphery, and the mid-peripheral nonperfusion emerged as a key factor for the development of neovascularization, consistent with previous studies suggesting that the mid-peripheral and far-peripheral retinal zones may be particularly sensitive to the impact of DR [4, 29, 30]. However, the literature is inconsistent in defining NPA localization, with some studies using radius-based definitions, while others adopt field-of-view concepts or the concentric ring method [24, 30, 31]. In this study, we adopted an anatomically guided approach to define retinal regions, using the fovea as the center and the distance to the optic disc as a reference for segmentation. This approach better captures the physiological relevance of topographic differences, defining the posterior pole as the area just beyond the disc and vascular arcades, and the mid-periphery as the region extending to the posterior edge of the vortex vein ampulla, consistent with the eye angle 130-degree field of view provided by our widefield OCTA [22, 32].

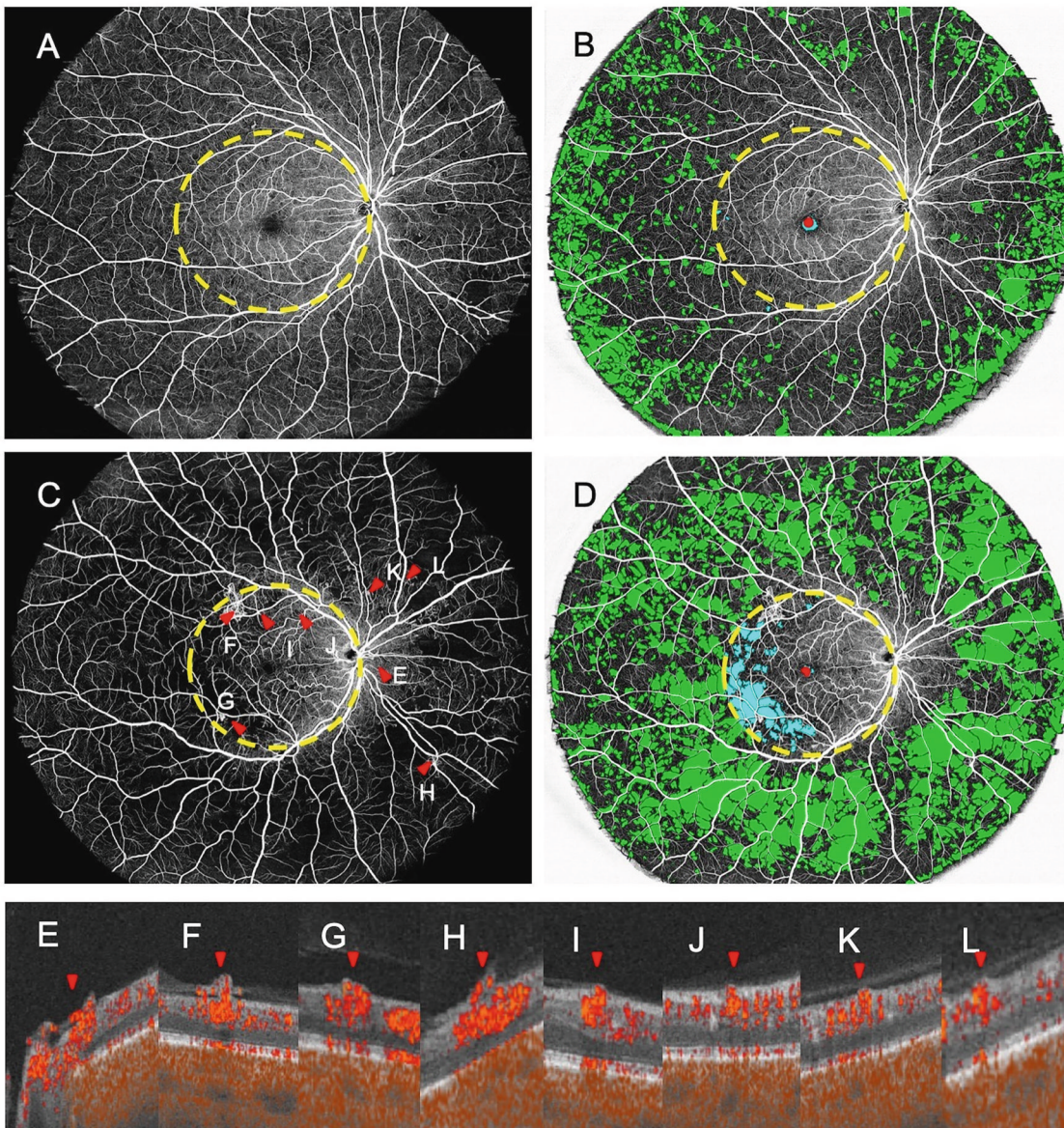


Fig. 1 Representative en face angiogram of the entire retinal layer from cases with and without subclinical retinal neovascularization (RNV). Images are divided into posterior pole and mid-peripheral regions, delineated by a yellow dashed circle centered on the fovea, with the radius determined by the distance from the fovea to the optic disc center. Nonperfusion area (NPA) in the posterior pole and mid-peripheral retina is coded in blue and green, and the foveal avascular zone in red, which is excluded from the NPA calculation. **A, B** En face angiogram and NPA map of a 50-year-old male with moderate NPDR and no subclinical RNV. **C, D** En face angiogram and NPA map of a 54-year-old male with severe NPDR showing RNVs (red arrows). **E–L** RNV is visualized in OCT B-scans with flow overlaid, showing abnormal flow signals breaching the internal limiting membrane.

In eyes with subclinical RNV, we observed significant differences in total and mid-peripheral NPA indices between eyes with NVD vs. those with NVE only. Previous FA-based and OCTA-based studies reported comparable findings [23, 33]. These findings may suggest that the presence of NVD is indicative of a more severe ischemia burden. This may also explain the long-established observation that eyes with NVD are at a greater risk for severe vision loss compared to eyes with NVE only [34]. Such cases may warrant closer monitoring and more aggressive treatment compared to eyes with NVE alone. However, the subgroup analysis comparing eyes with subclinical NVD and NVE alone was limited by small sample size. These preliminary findings should be further validated in larger cohorts.

Subclinical RNV can be understood as subclinical precursors to clinically evident RNV [11]. While clinical grading systems like the

ETDRS can estimate the short and long-term risk of proliferative disease, they are imprecise in that conversion to proliferative does not always go through stepwise progression, mild to moderate to severe NPDR, and even mild NPDR can progress to PDR in 1 year. We theorize that eyes with subclinical RNV are at a higher risk of developing clinically evident RNV for the same level of clinical retinopathy severity. By combining the detection of subclinical RNV and the quantification of NPA, we may be able to more precisely predict which eyes are at risk for developing vision-threatening retinopathy compared to clinical grading. For instance, eyes approaching or exceeding the 28.84% threshold could be presumed at higher risk for developing overt RNV compared to eyes with a much lower NPA index, even if both are clinically classified within the same DR severity stage. Such thresholds could indirectly influence treatment strategies by

Table 3. Comparison of retinal nonperfusion areas between eyes with and without subclinical RNV, and between eyes with subclinical NVD and subclinical NVE.

Parameter	RNV(+) (n = 14)	RNV(−) (n = 23)	P value	NVD (n = 7)	NVE (n = 7)	P value
Posterior NPA, %	3.49 ± 3.25	1.74 ± 2.11	0.328	4.77 ± 3.50	2.49 ± 2.75	0.147
mid-peripheral NPA, %	31.97 ± 7.02	24.80 ± 6.60	0.041	35.82 ± 5.86	29.48 ± 5.50	0.034
Total NPA, %	27.96 ± 6.36	21.61 ± 5.65	0.046	31.46 ± 4.93	25.67 ± 5.45	0.033

Continuous variables are expressed as mean ± standard deviation.

NPA nonperfusion area, NVD neovascularization of the optic disc, NVE neovascularization elsewhere, RNV retinal neovascularization.

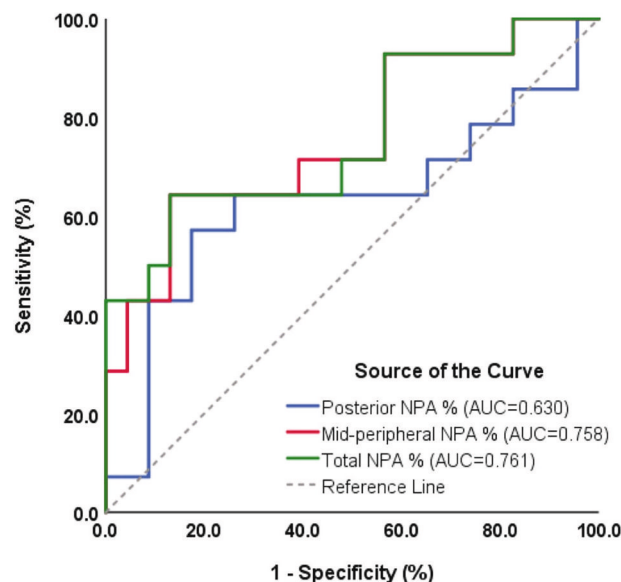


Fig. 2 Receiver operating characteristic curves for evaluating the predictive accuracy of the nonperfusion area (NPA) index in detecting subclinical retinal neovascularization (RNV). The green line represents the total NPA percentage ($AUC = 0.761$; 95% CI, 0.592–0.929), the red line represents the mid-peripheral NPA percentage ($AUC = 0.758$; 95% CI, 0.591–0.924), and the blue line represents the posterior NPA percentage ($AUC = 0.630$; 95% CI, 0.424–0.837).

identifying cases that may benefit from closer monitoring or earlier intervention. While these findings highlight the potential for subclinical RNV and NPA as a predictive biomarker, further larger and longitudinal studies are required to validate its prognostic utility and assess its role in guiding earlier interventions in DR.

This study has several limitations that should be considered. First, image distortion remains a confounding factor due to the curved retinal surface and the challenges of imaging the peripheral retina. This distortion may have affected measurements of peripheral capillary nonperfusion, particularly in eyes with longer axial lengths, posing challenges for accurate intercapillary distance measurements and NPA calculations [35]. To address this, we normalized NPAs using an index and defined retinal regions based on anatomical landmarks, such as the fovea and optic disc, ensuring anatomic region segmentation. However, future efforts to recognize and correct image distortion are necessary to improve measurement accuracy [36]. The resolution of the single-shot 26 × 21 mm OCTA scans is lower than that of scans of smaller fields of view, which may limit sensitivity to subtle microvascular abnormalities. Nonetheless, the broader field of view enabled a comprehensive assessment of ischemic changes across the retina. Additionally, not all cases were treatment naïve, and some subclinical RNV may represent regressed neovascularization following prior interventions. This highlights the need for refined

DR grading systems that account for documenting treatment responses, enabling a more accurate representation of disease severity and current activity [37]. Finally, the classification of DR severity in this study was based on clinical examination rather than standard 7-field color fundus photography or widefield imaging protocols. This may have contributed to an overestimation of the subclinical RNV detection rate by OCTA, as no ancillary widefield color imaging was used as a comparator. However, our approach reflects real-world clinical practice in assessing overall DR burden. Future longitudinal studies with larger cohorts and incorporation of multimodal widefield imaging are needed to validate the predictive value of NPA indices and further enhance the clinical utility of widefield OCTA in DR management.

In conclusion, this study demonstrates the utility of a widefield OCTA in detecting subclinical RNV and quantifying retinal NPAs in NPDR. By employing a single-shot imaging protocol and an anatomically guided approach to retinal region segmentation, we provided a comprehensive assessment of ischemic changes across the posterior and mid-peripheral retina. The identified NPA thresholds, particularly in the mid-peripheral region, highlight the potential of OCTA-derived metrics as predictive biomarkers for early proliferative changes.

SUMMARY

What was known before

- Previous research has demonstrated that OCTA can effectively identify an earlier form of RNV before it becomes clinically apparent.

What this study adds

- Single-shot widefield SS-OCTA demonstrates the capabilities of detecting subclinical RNV in a substantial proportion of eyes clinically graded as moderate to severe NPDR.
- A higher mid-peripheral NPA index correlates with subclinical RNV and may serve as a biomarker for identifying eyes at higher risk of developing PDR.

DATA AVAILABILITY

The datasets generated and analyzed in this study are available from the corresponding author upon reasonable request. Access may be subject to restrictions to protect patient confidentiality and institutional policy.

REFERENCES

- Lundein EA, Burke-Conte Z, Rein DB, Wittenborn JS, Saaddine J, Lee AY, et al. Prevalence of diabetic retinopathy in the US in 2021. *JAMA Ophthalmol.* 2023;141:747–54.
- Shaw JE, Sicree RA, Zimmet PZ. Global estimates of the prevalence of diabetes for 2010 and 2030. *Diabetes Res Clin Pract.* 2010;87:4–14.

3. Wykoff CC, Yu HJ, Avery RL, Ehlers JP, Tadayoni R, Sadda SR. Retinal non-perfusion in diabetic retinopathy. *Eye*. 2022;36:249–56.
4. Silva PS, Dela Cruz AJ, Ledesma MG, van Hemert J, Radwan A, Cavallerano JD, et al. Diabetic retinopathy severity and peripheral lesions are associated with nonperfusion on ultrawide field angiography. *Ophthalmology*. 2015;122:2465–72.
5. Lim JI, Kim SJ, Bailey ST, Kovach JL, Vemulakonda GA, Ying GS, et al. Diabetic retinopathy preferred practice pattern(R). *Ophthalmology*. 2025;132:P75–162.
6. Jia Y, Bailey ST, Hwang TS, McClintic SM, Gao SS, Pennesi ME, et al. Quantitative optical coherence tomography angiography of vascular abnormalities in the living human eye. *Proc Natl Acad Sci USA*. 2015;112:E2395–402.
7. Jia Y, Tan O, Tokayer J, Potsaid B, Wang Y, Liu JJ, et al. Split-spectrum amplitude-decorrelation angiography with optical coherence tomography. *Opt Express*. 2012;20:4710–25.
8. Hwang TS, Gao SS, Liu L, Lauer AK, Bailey ST, Flaxel CJ, et al. Automated quantification of capillary nonperfusion using optical coherence tomography angiography in diabetic retinopathy. *JAMA Ophthalmol*. 2016;134:367–73.
9. You QS, Guo Y, Wang J, Wei X, Camino A, Zang P, et al. Detection of clinically unsuspected retinal neovascularization with wide-field optical coherence tomography angiography. *Retina*. 2020;40:891–7.
10. Tsuboi K, Mazloumi M, Guo Y, Wang J, Flaxel CJ, Bailey ST, et al. Utility of en face OCT for the detection of clinically unsuspected retinal neovascularization in patients with diabetic retinopathy. *Ophthalmol Retina*. 2023;7:683–91.
11. Tsuboi K, Mazloumi M, Guo Y, Wang J, Flaxel CJ, Bailey ST, et al. Early sign of retinal neovascularization evolution in diabetic retinopathy: a longitudinal OCT angiography study. *Ophthalmol Sci*. 2024;4:100382.
12. Russell JF, Flynn HW Jr, Sridhar J, Townsend JH, Shi Y, Fan KC, et al. Distribution of diabetic neovascularization on ultra-widefield fluorescein angiography and on simulated widefield OCT angiography. *Am J Ophthalmol*. 2019;207:110–20.
13. Liang GB, Hormel TT, Wei X, Guo Y, Wang J, Hwang T, et al. Single-shot OCT and OCT angiography for slab-specific detection of diabetic retinopathy. *Biomed Opt Express*. 2023;14:5682–95.
14. Guo Y, Hormel TT, Gao L, You Q, Wang B, Flaxel CJ, et al. Quantification of nonperfusion area in montaged widefield OCT angiography using deep learning in diabetic retinopathy. *Ophthalmol Sci*. 2021;1:100027.
15. Wang J, Hormel TT, You Q, Guo Y, Wang X, Chen L, et al. Robust non-perfusion area detection in three retinal plexuses using convolutional neural network in OCT angiography. *Biomed Opt Express*. 2020;11:330–45.
16. Wilkinson CP, Ferris FL 3rd, Klein RE, Lee PP, Agardh CD, Davis M, et al. Proposed international clinical diabetic retinopathy and diabetic macular edema disease severity scales. *Ophthalmology*. 2003;110:1677–82.
17. Guo Y, Camino A, Zhang M, Wang J, Huang D, Hwang T, et al. Automated segmentation of retinal layer boundaries and capillary plexuses in wide-field optical coherence tomographic angiography. *Biomed Opt Express*. 2018;9:4429–42.
18. Hormel TT, Wang J, Bailey ST, Hwang TS, Huang D, Jia Y. Maximum value projection produces better en face OCT angiograms than mean value projection. *Biomed Opt Express*. 2018;9:6412–24.
19. Guo Y, Camino A, Wang J, Huang D, Hwang TS, Jia Y. MEDnet, a neural network for automated detection of avascular area in OCT angiography. *Biomed Opt Express*. 2018;9:5147–58.
20. Guo Y, Hormel TT, Xiong H, Wang B, Camino A, Wang J, et al. Development and validation of a deep learning algorithm for distinguishing the nonperfusion area from signal reduction artifacts on OCT angiography. *Biomed Opt Express*. 2019;10:3257–68.
21. Guo Y, Hormel TT, Gao M, You Q, Wang J, Flaxel CJ, et al. Multi-plexus non-perfusion area segmentation in widefield OCT angiography using a deep convolutional neural network. *Transl Vis Sci Technol*. 2024;13:15.
22. Choudhry N, Duker JS, Freund KB, Kiss S, Querques G, Rosen R, et al. Classification and guidelines for widefield imaging: recommendations from the International Widefield Imaging Study Group. *Ophthalmol Retina*. 2019;3:843–9.
23. Nicholson L, Ramu J, Chan EW, Bainbridge JW, Hykin PG, Talks SJ, et al. Retinal nonperfusion characteristics on ultra-widefield angiography in eyes with severe nonproliferative diabetic retinopathy and proliferative diabetic retinopathy. *JAMA Ophthalmol*. 2019;137:626–31.
24. Yu G, Aaberg MT, Patel TP, Iyengar RS, Powell C, Tran A, et al. Quantification of retinal nonperfusion and neovascularization with ultrawidefield fluorescein angiography in patients with diabetes and associated characteristics of advanced disease. *JAMA Ophthalmol*. 2020;138:680–8.
25. Nakao S, Yoshida S, Kaizu Y, Yamaguchi M, Wada I, Ishibashi T, et al. Microaneurysm detection in diabetic retinopathy using OCT angiography may depend on intramicroaneurysmal turbulence. *Ophthalmol Retina*. 2018;2:1171–3.
26. Zhang M, Hwang TS, Dongye C, Wilson DJ, Huang D, Jia Y. Automated quantification of nonperfusion in three retinal plexuses using projection-resolved optical coherence tomography angiography in diabetic retinopathy. *Invest Ophthalmol Vis Sci*. 2016;57:5101–6.
27. Campbell JP, Zhang M, Hwang TS, Bailey ST, Wilson DJ, Jia Y, et al. Detailed vascular anatomy of the human retina by projection-resolved optical coherence tomography angiography. *Sci Rep*. 2017;7:42201.
28. You QS, Wang J, Guo Y, Pi S, Flaxel CJ, Bailey ST, et al. Optical Coherence tomography angiography avascular area association with 1-year treatment requirement and disease progression in diabetic retinopathy. *Am J Ophthalmol*. 2020;217:268–77.
29. Shimizu K, Kobayashi Y, Muraoka K. Midperipheral fundus involvement in diabetic retinopathy. *Ophthalmology*. 1981;88:601–12.
30. Wang F, Saraf SS, Zhang Q, Wang RK, Rezaei KA. Ultra-widefield protocol enhances automated classification of diabetic retinopathy severity with OCT angiography. *Ophthalmol Retina*. 2020;4:415–24.
31. Nicholson L, Vazquez-Alfageme C, Ramu J, Triantafyllopoulos I, Patrao NV, Muwas M, et al. Validation of concentric rings method as a topographic measure of retinal nonperfusion in ultra-widefield fluorescein angiography. *Am J Ophthalmol*. 2015;160:1217–25.e2.
32. Quinn N, Csincsik L, Flynn E, Curcio CA, Kiss S, Sadda SR, et al. The clinical relevance of visualising the peripheral retina. *Prog Retin Eye Res*. 2019;68:83–109.
33. Stino H, Huber KL, Niederleithner M, Mahnert N, Sedova A, Schlegl T, et al. Association of diabetic lesions and retinal nonperfusion using widefield multimodal imaging. *Ophthalmol Retina*. 2023;7:1042–50.
34. Rand LI, Prud'homme GJ, Ederer F, Canner PL. Factors influencing the development of visual loss in advanced diabetic retinopathy. *Diabetic Retinopathy Study (DRS) Report No. 10*. *Investig Ophthalmol Vis Sci*. 1985;26:983–91.
35. Tan CS, Chew MC, van Hemert J, Singer MA, Bell D, Sadda SR. Measuring the precise area of peripheral retinal non-perfusion using ultra-widefield imaging and its correlation with the ischaemic index. *Br J Ophthalmol*. 2016;100:235–9.
36. Mehta N, Cheng Y, Alibhai AY, Duker JS, Wang RK, Waheed NK. Optical coherence tomography angiography distortion correction in widefield montage images. *Quant Imaging Med Surg*. 2021;11:928–38.
37. Wong TY, Sun J, Kawasaki R, Ruamviboonsuk P, Gupta N, Lansingh VC, et al. Guidelines on diabetic eye care: The International Council of Ophthalmology recommendations for screening, follow-up, referral, and treatment based on resource settings. *Ophthalmology*. 2018;125:1608–22.

AUTHOR CONTRIBUTIONS

AW designed the methodology, collected data, conducted analysis, interpreted results, and drafted the original manuscript. YG contributed to data review, analysis, and result interpretation. TTH provided critical manuscript revisions. CJF, MT, STB, and DP assisted with data collection, offered clinical insights, and reviewed and edited the manuscript. YJ provided expertise in OCTA, contributed to study design and data interpretation, and critically revised the manuscript. TSH conceptualized the study, supervised the research process, interpreted results, and provided critical revisions and final approval. All authors reviewed and approved the final manuscript.

FUNDING

This work was supported by grants from National Institutes of Health (R01 EY 036429, R01 EY035410, R01 EY024544, R01 EY027833, R01 EY031394, R43EY036781, P30 EY010572, T32 EY023211, UL1TR002369); the Jennie P. Weeks Endowed Fund; the Malcolm M. Marquis, MD Endowed Fund for Innovation; Unrestricted Departmental Funding Grant and Dr. H. James and Carole Free Catalyst Award from Research to Prevent Blindness (New York, NY); Edward N. & Della L. Thome Memorial Foundation Award, and the Bright Focus Foundation (G2020168, M20230081). The funding source had no role in the design and conduct of the study; collection, management, analysis, and interpretation of the data; preparation, review, or approval of the manuscript; and decision to submit the manuscript for publication.

COMPETING INTERESTS

YG: Visionix/Optovue (P), Genentech (R), Ifocus Imaging (P); TTH: Ifocus Imaging (I); STB: Visionix/Optovue (F); YJ: Visionix/Optovue (P, R), Roche/Genentech (P, R, F), Ifocus Imaging (I, P), Optos (P), Boeringer Ingelheim (C), Kugler (R). These potential conflicts of interest have been reviewed and managed by OHSU. Other authors declare no conflicts of interest related to this article.

ADDITIONAL INFORMATION

Supplementary information The online version contains supplementary material available at <https://doi.org/10.1038/s41433-025-03891-2>.

Correspondence and requests for materials should be addressed to Thomas S. Hwang.

Reprints and permission information is available at <http://www.nature.com/reprints>

Publisher's note Springer Nature remains neutral with regard to jurisdictional claims in published maps and institutional affiliations.

Springer Nature or its licensor (e.g. a society or other partner) holds exclusive rights to this article under a publishing agreement with the author(s) or other rightsholder(s); author self-archiving of the accepted manuscript version of this article is solely governed by the terms of such publishing agreement and applicable law.